AD-A157 554 THE MEASUREMENTS OF AXISYMMETRIC AIR TURBULENT JET FLOW 1/1
WITH AN INDIVIDUA..(U) FOREIGN TECHNOLOGY DIV
WRIGHT-PATTERSON AFB OH X SHEN ET AL. 29 MAY 85
UNCLASSIFIED FTD-ID(RS)T-0326-85 F/G 14/2 NL

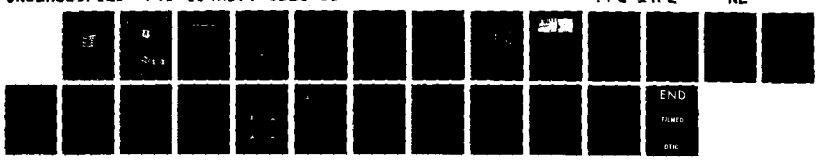

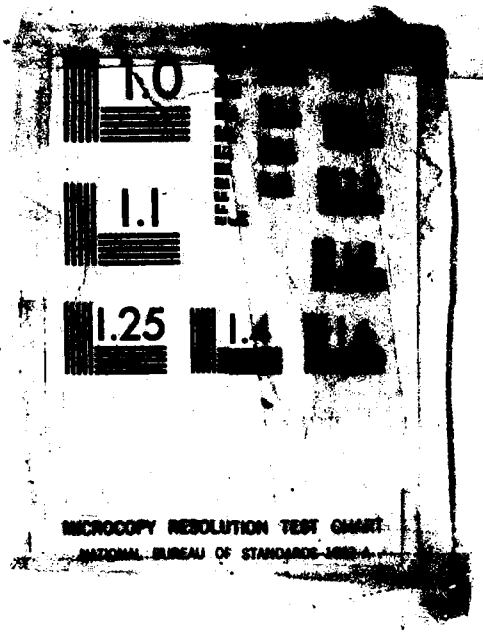
1.0
1.1
1.25
1.4
MICROCOPY RESOLUTION TEST CHART
NATIONAL BUREAU OF STANDARDS-1963-A

FTD-ID(RS)T-0326-85

AD-A157 554

FOREIGN TECHNOLOGY DIVISION

THE MEASUREMENTS OF AXISYMMETRIC AIR TURBULENT JET FLOW WITH AN INDIVIDUAL REALIZATION LASER VELOCIMETER SYSTEM

by

Shen Xiong, Yu. Hesheng, et al.

DTIC FILE COPY

DTIC
ELECTE
S JUL 19 1985 D
G

Approved for public release;
distribution unlimited.

85 6 28 137

EDITED TRANSLATION

FTD-ID(RS)T-0326-85 29 May 1985

MICROFICHE NR: FTD-85-C-000363

THE MEASUREMENTS OF AXISYMMETRIC AIR TURBULENT JET FLOW WITH AN INDIVIDUAL REALIZATION LASER VELOCIMETER SYSTEM

By: Shen Xiong, Yu. Hesheng, et al.

English pages: 20

Source: Qinghua Daxue Xuebao, Vol. 24, No. 3, 1984, pp. 26-36

Country of origin: China
Translated by: FLS, INC.
F33657-85-D-2079
Requester: FTD/TQIA
Approved for public release; distribution unlimited.

THIS TRANSLATION IS A RENDITION OF THE ORIGINAL FOREIGN TEXT WITHOUT ANY ANALYTICAL OR EDITORIAL COMMENT. STATEMENTS OR THEORIES ADVOCATED OR IMPLIED ARE THOSE OF THE SOURCE AND DO NOT NECESSARILY REFLECT THE POSITION OR OPINION OF THE FOREIGN TECHNOLOGY DIVISION.

PREPARED BY:

TRANSLATION DIVISION
FOREIGN TECHNOLOGY DIVISION
WP-AFB, OHIO.

GRAPHICS DISCLAIMER

All figures, graphics, tables, equations, etc. merged into this translation were extracted from the best quality copy available.

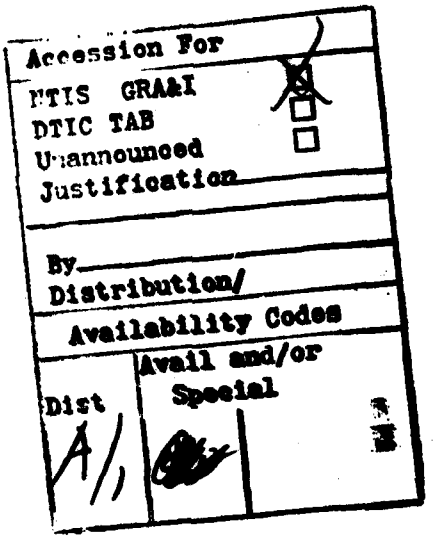

The Measurements of Axisymmetric Air Turbulent Jet Flow with an Individual Realization Laser Velocimeter System

Shen Xiong, Yu Hesheng, Dept. of Engineering Mechanics, Tsinghua University; Chen Dianlan, Xie Suhuan, Dept. of Mechanics, Beijing University

ABSTRACT

This paper describes the measurements of axisymmetric air turbulent jet flow with the use of an IRLV system. The distributions of axial mean velocity, turbulent intensity and probability density functions of velocity in the initial region of jet flow were obtained. The data from LV were sampled and processed automatically by a microprocessor. The experiments show that the velocity measurements can be realized even with the air particles in their natural state. The measurements of the mean velocity were also simultaneously made with a hot wire anemometer in order to compare with those made with a LV. Their results were in good coincidence in the core flow region. The velocity bias was increased with the decrease of data rate and increase of turbulent intensity in the mixing boundary layer. Keywords: Laser velocimeters (LV), velocity measurements. (Translations)

Key words: jet flow, laser,

I. Introduction

One of the important milestones in the development of laser velocimetry techniques in recent years is the increasing popularity of the IRLV [Individual Realization Laser Velocimeter][1]. The feature of this technique is its incorporation of a dual-beam fringe mode optical device, which includes a large aperture

receiving lens, with an individual realization counter-type Doppler signal processor. Since this system works well for sparsely seeded flow, it is especially suited for gas flow velocity measurements. The counter-type signal processor has direct digital output. Thus, data analysis can be accomplished without analog-to-digital conversion. The output is directly fed into the microprocessor to obtain various statistical parameters relevant to the flow.

This paper described the measurements of axisymmetric air turbulent jet flow with the use of an IRLV system. The mean velocity distribution was also measured simultaneously with a hot wire anemometer for comparison purposes. The light source used was a small power He-Ne laser. In most cases, particle seeding is not necessary and velocity measurements can be realized with air particles in their natural state. It is productive, however, to introduce a small quantity of particles into the flow if a higher data rate is desired for the purpose of shortening the measurement time, and thereby obtaining more reliable statistical data. The IRLV system is different from the frequency tracker in that the latter basically performs under the condition of continuous signals. Therefore, experimental conditions and experimenter's techniques as well as judgment on certain experiment phenomena will significantly affect measurements using the IRLV system. Despite numerous theories and methods for adjusting bias [2,3], the IRLV measurements could vary considerably under different conditions. Consequently, data analysis of the IRLV system is an important subject which has motivated many research activities.

II. Experimental Systems and Measurement Techniques

Figure 1 and Fig. 2 show the experimental systems which consist of the model, IRLV system and hot wire anemometer.

1. Flow system

The flow system is composed of the jet flow model, fan and atomizer, etc. The jet nozzle diameter, D, is 38 mm. A beehive stablizer and two layers of mesh are positioned near the entrance of the convergent section. The fan is controlled by the rheostat to attain desired air velocity. Mean air velocity reaches 15 m/sec at a maximum fan speed. Two air velocities, 4.53 m/sec and 14.33 m/sec, were selected to conduct measurement, and the corresponding Reynolds numbers are 1.15×10^4 and 3.63×10^4, both within the turbulent flow range.

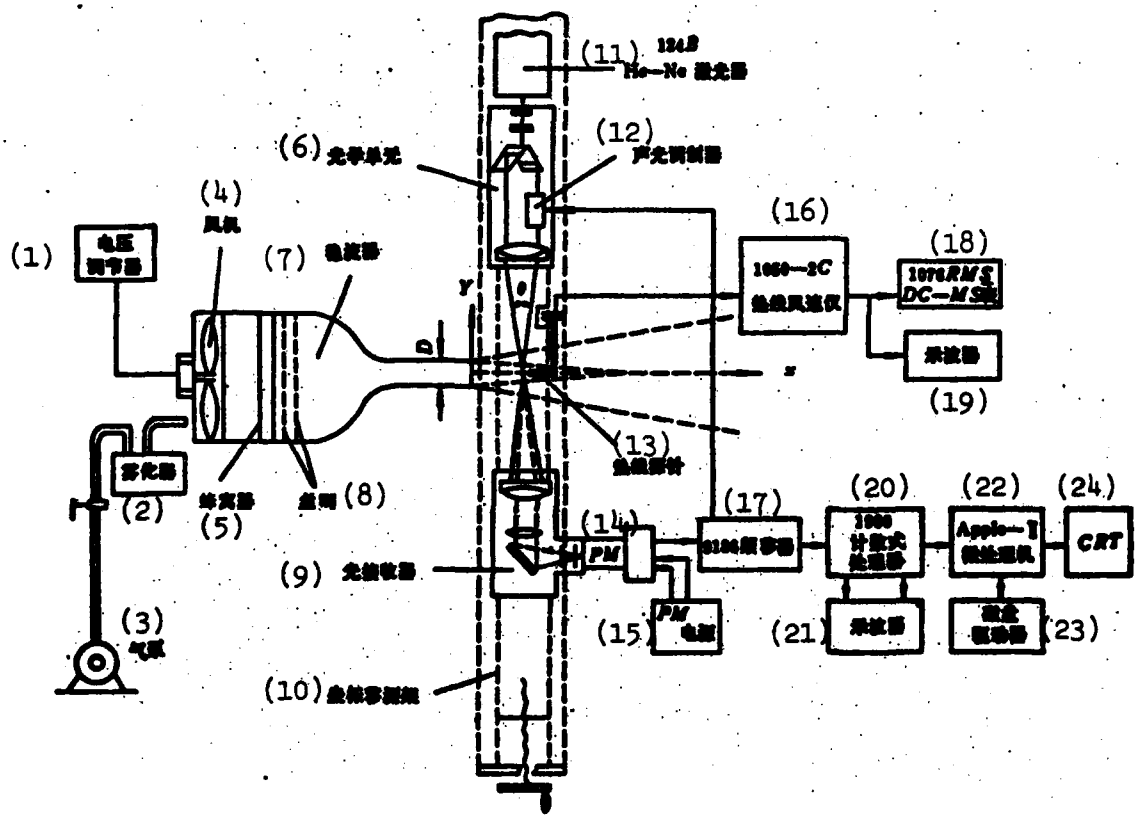

Fig. 1 Schematic diagram of the experimental apparatuses and measurement systems.
Key: (1) Rheostat; (2) Atomizer; (3) Pump; (4) Fan (5) Beehive; (6) Optical unit; (7) Stablizer; (8) Mesh; (9) Scattered light receiver; (10) Traverse rod; (11) He-Ne laser; (12) Acousto-optic cells; (13) Hot wire probe; (14) Photomultiplier; (15) Power supply; (16) Hot wire anemometer; (17) Frequency shifter; (18) DC-MS gauge; (19) Oscilloscope; (20) Counter-type processor; (21) Oscilloscope; (22) Microprocessor; (23) Disc drive; (24) Cathode ray tube.

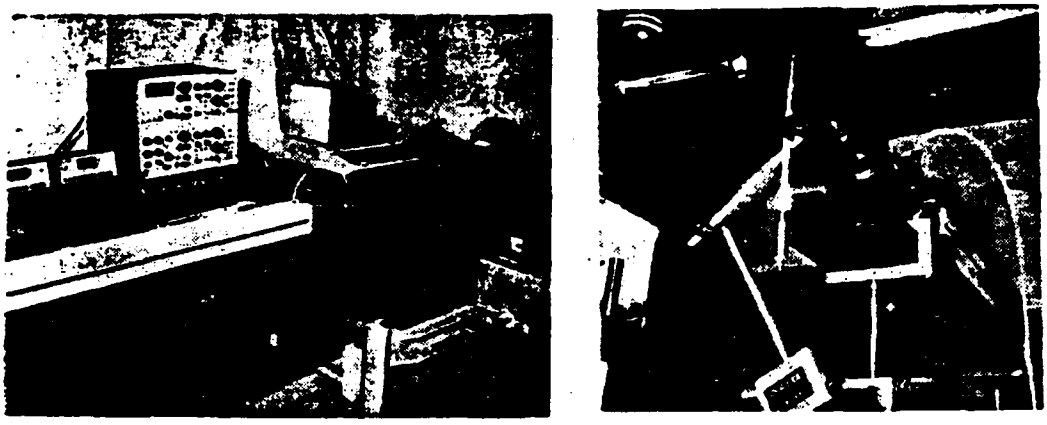

(a) 全貌　　(b) 测量区局部放大

Fig. 2 Experimental apparatus and instrument set-up

Key: (a) Overview; (b) Close-up of the measurement devices

The atomizer generates light scattering particles used in this experiment. Atomization is achieved by employing compressed air to break water into droplets of a diameter in the microns and subsequently introducing them into the air stream. Particle number density can be altered by changing the compressed air pressure. In fact, this experiment could have been conducted using only the natural particles in the indoor air. However, the data rate obtained would have been lower, usually between 100 Hz~300 Hz and longer measurement time would have been required in order to obtain a set amount of validated data.

The axial orientations of the free jet flow have been specified in Fig. 1. The distribution of horizontal axial (x-direction) mean velocity and turbulent intensity were measured. The optical system and hot wire probe were mounted on the same traverse rod with the hot wire probe located 2 mm below the optical control volume to avoid longitudinal time lag.

2. LDV Optical System

The LDV Laser Doppler Velocimeter optical system consists of laser, optical unit (including acousto-optic cells) and light receiver and was arranged according to the 9100-3 type optical circuit [10]. The components and their basic parameters are as follows:

The He-Ne laser power output is 15 mW, single mode with laser beam wave length $\lambda = 0.6328 \times 10^{-3}$ mm. The optical unit is composed of half-wave plate, beam splitter, and transmitting lens. The acousto-optic cells are used to obtain optical frequency shift. It is especially useful when flow reversal occurs and it also helps to eliminate "fringe bias" caused by radial velocity. For free jet flow, however, radial velocity components are small and there is practically no flow reversal in its core flow region; therefore, frequency shift is not really necessary. Moreover, since the hot wire anemometer simultaneously used in this experiment is insensitive to flow direction, the acousto-optic cells were thus not used, which also reduced laser power loss.

The control volume parameters are defined by beam separation and transmitting lens focal length of the optical unit. In this system:

Beam separation d=50 mm

Transmitting lens focal length f=250 mm

Transmitting beam $\frac{1}{e^2}$ intensity diameter De^{-2} =1.1 mm

Thus, half angle of the incidence angle $\theta/2=5.71°$. Using the following formula:

$$f_D=\frac{2\sin\theta/2}{\lambda}|U_s|$$

The frequency-velocity conversion coefficient can be calculated $C_{f\to v}=\frac{\lambda}{2\sin\theta/2}=3.18\frac{m/sec}{MHz}=3.18\mu m$. For fringe mode, this is also the spacing, d_f, of fringes in the control volume. The dimensions of the control volume can also be determined, i.e. width d_m=0.18 mm and length l_m=1.8 mm. Thus, the number of fringes, N_f, in the control volume is calculated to be 56.6.

The receiving lens is of the forward-scatter type. Since the larger lens aperture (D_a=50 mm) increases scattered light intensity, and therefore photomultiplier quantum efficiency (η=0.21), a larger signal-to-noise ratio is obtained.

3. Estimate of Signal-to-Noise Ratio

The signal-to-noise ratio (SNR) of single particle burst signals can be estimated as follows[5]:

$$SNR=4\times10^{-11}\frac{\eta P_0}{\Delta f}\left[\frac{D_a}{r_a}\ \frac{D_a^{-2}}{f}\right]^2 d_p^2 G^2$$

where: η - photomultiplier quantum efficiency,

P_0 - power of each light beam,

d_p - particle diameter,

$\bar{V}$ - fringe visibility,

$\bar{G}$ - scattering function,

Δf - test band width,

D_e^{-2} - test beam $\frac{1}{e^2}$ intensity diameter,

f - transmitting lens focal length,

r_a - receiving lens focal length,

D_a - receiving lens aperture.

At 10 MHz band width SNR is calculated to be about 9 dB for particles of 1 μm in diameter. Although this is only an estimation, it shows that, under ideal conditions, maximum value of SNR can be reached. During the experiment the burst signals on the oscilloscope were clear, which indicated that the true SNR was close to the above estimation.

4. Processing of Doppler Signals

Photoelectric signals from the photomultiplier were first fed into an amplifier for signal enhancement before being processed in the TSI1980 counter-type processor[10]. If the frequency shifter had been added, the signals would have been mixed at the frequency shifter to obtain the required amount of frequency shift and then processed at the signal processor.

The counter-type processor is capable of working under both N cycle comparison mode and full burst mode with the latter being

ore suitable for situations where lateral velocity causes serious ringe bias. Since in free jet flow the axial velocity component is uch larger than the radial velocity component, fringe bias is of ittle significance. Consequently, the N cycle comparison mode was elected for this experiment with cycle number set at 16 and omparison accuracy at 4%. With this arrangement both accuracy and equired measurement time had been properly taken into onsideration.

The timer unit of the processor measures, through counting nd comparison, the envelopment time of N Doppler cycles. This easurement is converted into a 16-bit word (12 bits are fractions nd 4 bits are exponents) binary output; or, through nalog-to-digit conversion, displayed on the simulated voltmeter of he readout unit. Since this measured time is inversely roportional to Doppler frequency, the higher the frequency (higher low velocity), the smaller the measurement (lower flow velocity). n order to obtain better signal resolution, and yet still within he measuring span, proper selection of the index span is ssential. When a microprocessor data collection system is used, he automatic span-set process mode should be selected with the pan index set at the maximum position. However, if the readout isplay unit is used, then the manual span-set process mode must be mployed to manually adjust the index span according to the magni- ude of measured value. Improper adjustment will result in easurement errors.

5. Automatic Data Collection and Processing

A TSI1980 counter-type processor coupled with an APPLE II microcomputer data collection and processing system[10] contains 48 K memory. Using special programming, the numerical data from the signal processor were collected and processed on the microprocessor to obtain velocity probability density function, mean velocity and local turbulent intensity. There are two kinds of data collection methods: time-averaging selection and random (Handshake) selection.

One of the advantages of the counter-type processor is that its validated data points occur randomly and are discontinuous. Accordingly, the sampling method, volume and interval (for equal internal sampling) must be carefully selected in accordance with flow character and data rate, etc. to obtain a correct statistical analysis.

The velocity probability density can be estimated from the time span of the sampling points as follows:

$$p[V, W] = P_{rob.}\left[\left(V - \frac{W}{2}\right) < V(t) < \left(V + \frac{W}{2}\right)\right]$$

$$= \frac{1}{N}\sum_i \Delta N_i \times 100\%$$

where: N is sampling volume, ΔN_i is number of data points with velocity between $\left(V - \frac{W}{2}\right)$ and $\left(V + \frac{W}{2}\right)$, and W is coordinate scale which is directly related to resolution of velocity measurement.

Mean velocity is estimated as:

$$\bar{V} = \frac{1}{N} \sum_{i=1}^{N} V_i$$

Local turbulent intensity is estimated as:

$$T.I. = \frac{1}{\bar{V}} \sqrt{\frac{N \sum_{i=1}^{N} V_i^2 - \left(\sum_{i=1}^{N} V_i \right)^2}{N(N-1)}}$$

For the IRLV system, the data acquisition rate is closely related to mean velocity, velocity fluctuations and particle distribution, etc. When the data rate is low and variant, the number of validated data points in the same sampling interval may vary substantially if the time-averaging selection method is used. However, this is not the case if the random selection method is employed, as it requires that a sufficient number of data points be reached before the sampling process is completed. Total sampling time varies with the different data rate.

The disadvantage of the random selection method is that the randomly sampled burst signals cause particle velocity bias. Correction for total velocity bias must be considered under flow conditions of a high turbulent intensity and a low data rate. Bias correction was not taken into consideration in the data analysis of this experiment and thus errors might result. These potential errors will be further discussed in the next section.

III. Results and Discussion

1. Axial Mean Velocity and Turbulent Intensity Distributions

Figure 3 shows, under two different Reynolds numbers, distributions of axial mean velocity and turbulent intensity near the jet core flow region. The dashed lines represent mean velocity distributions measured by hot wire anemometer. For easy comparison the measured axial mean velocity was normalized with respect to jet exit centerline axial mean velocity.

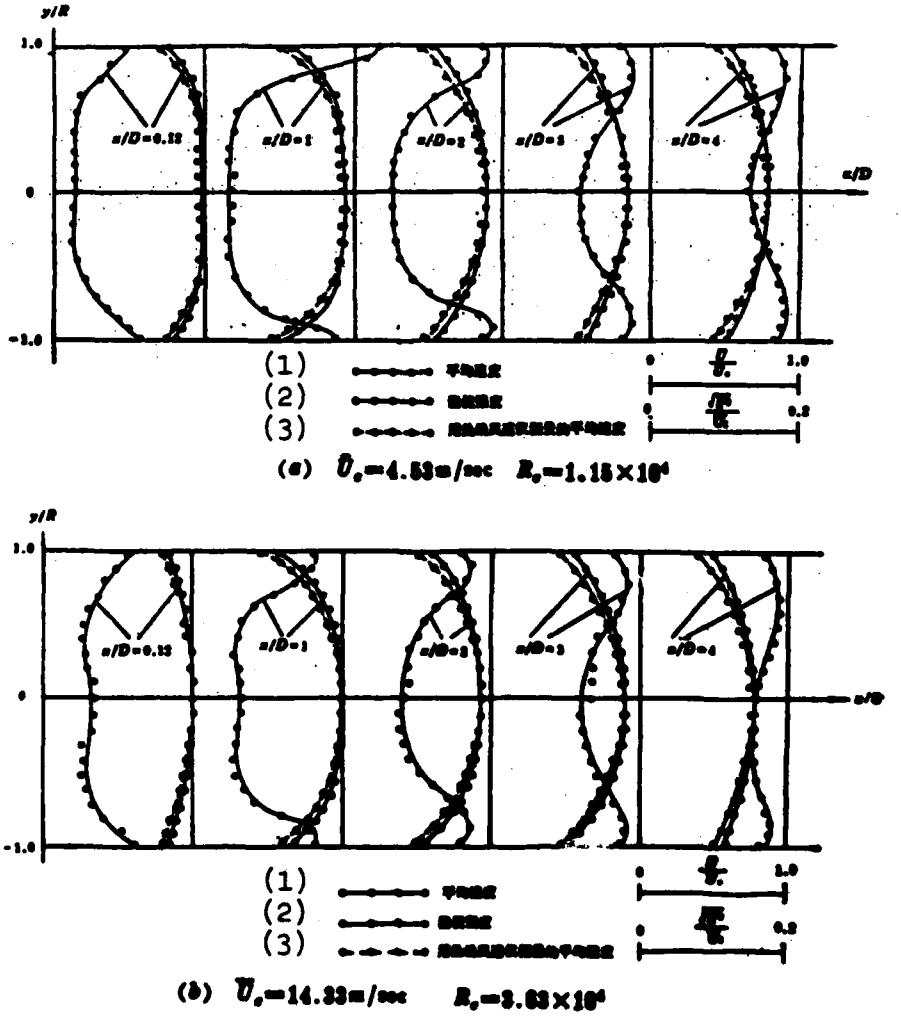

Fig. 3 Axial mean velocity and turbulent intensity distributions in the initial region of axisymmetric jet flow
Key: (1) Mean velocity; (2) Turbulent intensity; (3) Mean velocity measurements by hot wire anemometer.

It can be seen that initially there is a core flow region with low turbulent intensity and the relatively mean velocity in the core region remains unchanged[6]. Since momentum and mass transfer take place in the core region initially, a boundary layer of a certain thickness is formed. The thickness of this boundary layer increases, and thus the core flow region decreases, as the distance from the jet exit increases. Axial velocity in the core region tends to decrease slightly. Turbulent intensity varies inversely with changes in mean velocity. Near the symmetric axis, turbulent intensity is small whereas it increases significantly in the boundary layer until a peak value is reached. While the turbulent intensity gradient levels off as the jet flow moves forward, the turbulent intensity at each cross section of the jet flow keeps increasing and it is higher at high flow velocity than that at low velocity. Figure 4 represents distributions of axial mean velocity and local turbulent intensity along 75% radius line with $\bar{U}_c$=14.33 m/sec. Compared with results obtained under similar conditions[9], the turbulent intensity level appears higher and is not uniformly distributed. It is estimated that the discrepencies are caused by the fan.

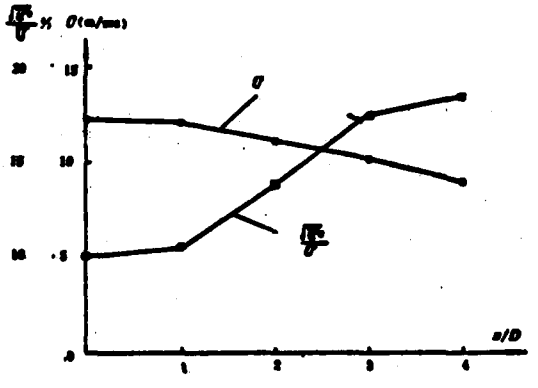

Fig.4 Distributions of jet flow axial mean velocity and local turbulent intensity along 75% radius line (jet exit centerline mean velocity $\bar{U}_c$=14.33 m/sec.

2. Axial Velocity Probability Density Functions

Figures 5, 6, and 7 show axial velocity probability density functions of several representative measurement points in the flow field. The locations of measurement points are shown in Fig. 8.

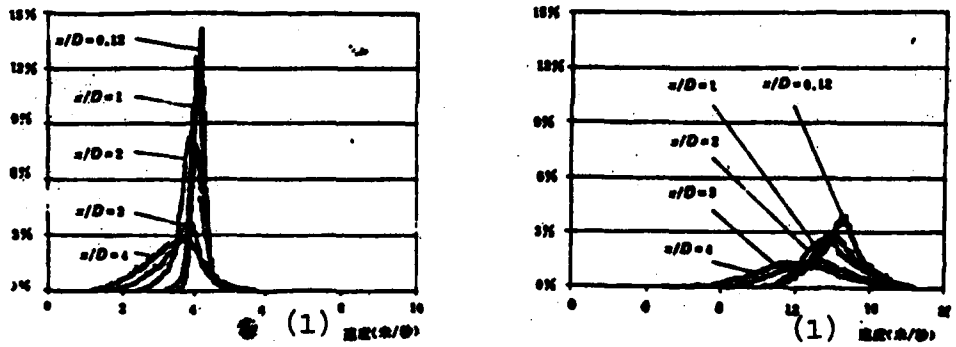

(a) $\bar{U}_c$=4.53 米/秒(2) (b) $\bar{U}_c$=14.33 米/秒(2)

Fig. 5 Centerline axial velocity probability density functions
Key: (1) Velocity (m/sec); (2) m/sec.

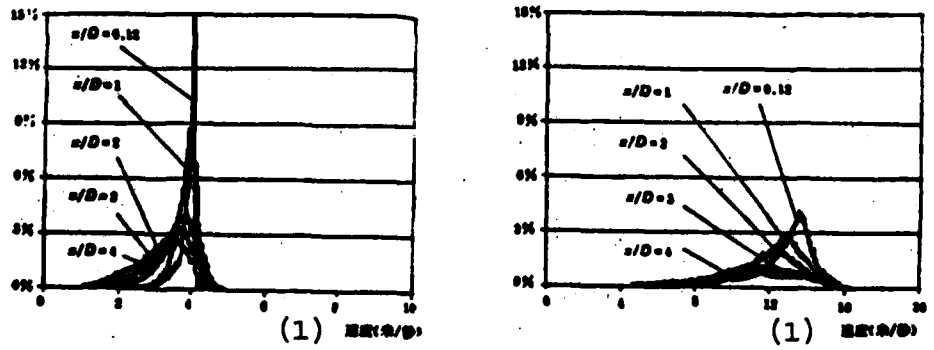

(a) $\bar{U}_c$=4.53 米/秒 (2) (b) $\bar{U}_c$=14.33 米/秒 (2)

Fig. 6 Axial velocity probability density functions along 75% radius line
Key: (1) Velocity (m/sec); (2) m/sec.

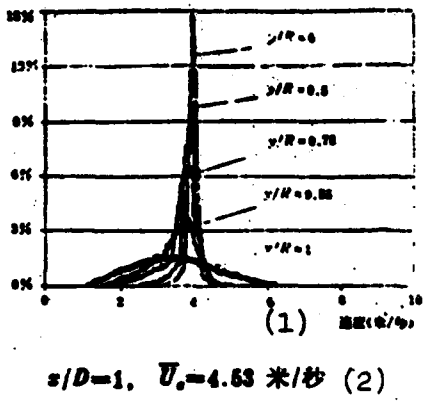

$x/D=1$, $\overline{U}_e=4.63$ 米/秒

Fig. 7 Axial velocity probability density functions along radial direction
Key: (1) Velocity (m/sec); (2) m/sec.

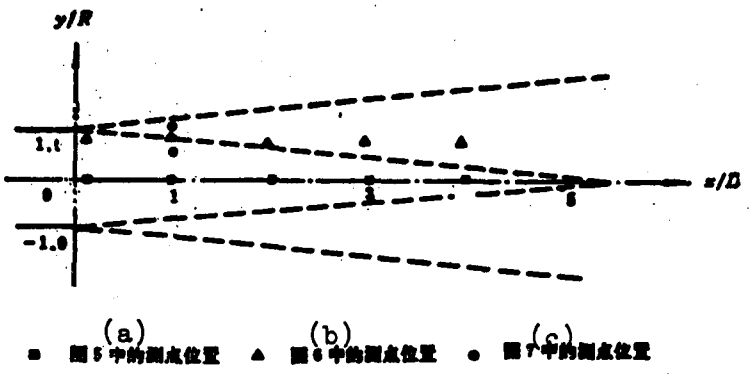

Fig. 8 Representative locations of measurement points for axial velocity probability density functions
Key: (a) Measurement points location in Fig. 5; (b) Measurement points location in Fig. 6; (c) Measurement points location in Fig. 7.

Figure 5(a) and 5(b) each represent the profiles of centerline axial velocity probability density functions at different flow velocity. The profiles are essentially symmetric and they rise sharply with a narrow width near the jet exit indicating low turbulent intensity. As the jet moves forward, the velocity fluctuation increases significantly. At higher flow velocity the velocity fluctuations near the jet exit are quite large as compared with those at low flow velocity, and consequently the turbulent intensity level of the entire flow field is higher.

Figure 6(a) and 6(b) represent, at two different flow velocities, axial velocity probability density functions along the 75% radius line in the boundary layer. The density functions for those points located near the side of greater velocity gradient in the boundary layer main flow region are markedly offset with a negative offset coefficient. This reflects the characteristics of

velocity fluctuations in the boundary layer and is consistent with results reported in other literature[7].

Figure 7 shows the profiles of axial velocity probability density functions at a downstream distance of x/D=1. It can be seen that velocity fluctuation increases rapidly as y/R increases. At y/R=1, local turbulent intensity reaches 33.6%. Such a high intensity is difficult to measure with other methods.

3. Velocity Bias

The factors which cause bias in the IRLV system are complex. Generally speaking, velocity bias occurs because the probability of particles with different velocity passing through the control volume is different. Even with uniform seeding, more high-velocity particles will pass through the control volume than do low-velocity particles. Obviously, only in stable laminar flow can there be no bias effects. If all Doppler burst signals received by the processor are validated, then the arithmetic average of such a data group will be greater than the true mean velocity. With random velocity fluctuations, the correct mean velocity can be calculated by taking the arithmetic average of velocities measured by the time-averaging method. This, however, can only be achieved at a very high particle number density.

So, what are the factors that affect velocity bias at a low particle number density? Reference [8] reported the analytical and

experimental study of statistical bias using subsonic air jet flow with the IRLV system and concluded that numerous factors would affect the magnitude of bias. For example, proper selection of the sampling rate per primary flow frequency and the data processing rate may reduce bias. Particle number density-velocity correlations also significantly alter bias. Accordingly, the cumulative effects of several mechanisms might reduce the magnitude of bias. Unfortunately, certain bias correction procedures are now being routinely employed even before significant bias in the data is identified. This, of course, can lead to even more errors. It was reported in Reference [9] that the experiment using velocity bias and time-averaging to correct for turbulent intensity resulted in complete opposite effects. In the jet flow core region, however, results of LV [Laser Velocimeter] and HW [Hot Wire] coincided well.

In order to study the effects of bias, a hot wire anemometer was used simultaneously in this experiment. A Model 1125 calibrator was used to calibrate the hot wire anemometer before the experiment and an accuracy of 1% was attained[11]. As shown in Fig. 3, the measurements of both LV and HW in the core flow region coincided very well. In the boundary layer, however, the measured values of IRLV were higher than those of HW. This discrepancy was attributed to bias caused by increasing turbulent intensity and decreasing data rate in this region. Figure 9 shows the correlations between measured data rates along radial direction on the X/D=2 cross-section and relative velocity bias $\Delta\% = \frac{U_{LV} - U_{HW}}{U_{HW}} \times 100\%$,

where $\bar{U}_{LV}$ and $\bar{U}_{HW}$ are the measured mean velocities using LV and HW, respectively. Data were randomly sampled. Sampling volume N=1000 was used to estimate mean velocity and turbulent intensity. Under given conditions, the sampling time needed was about 10 seconds and the statistical analysis time was about 20 seconds. Experiment results showed that these time selections were appropriate. If reducing bias is desired, it is necessary to either modify the data deduction procedures or increase the particle number density in order to increase data rate.

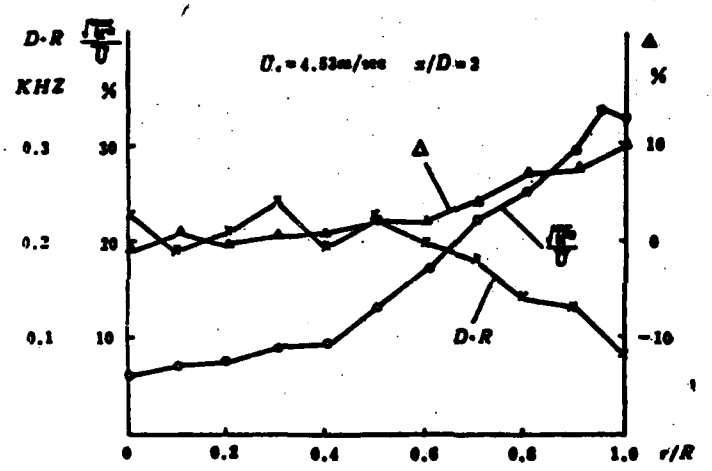

Fig. 9 Correlations between local turbulent intensity, data rate and relative bias error (Δ) along radial direction ($\Delta=\frac{\bar{U}_{LV}-\bar{U}_{HW}}{\bar{U}_{HW}}\times 100\%$).

IV. Concluding Remarks

Experimental results and analyses show that it is very convenient to employ the IRLV system to measure gas flow velocity. Normally, velocity measurements can be realized even with only air particles in their natural state as long as sufficient SNR is attained. It is important to properly select optical parameters, signal processor functions and

sampling parameters according to particles in their natural state as long as sufficient SNR is attained. It is important to properly select optical parameters, signal processor functions and sampling parameters according to flow structure for making measurements at low particle number density. Generally speaking, the statistical analyses are more reliable with low turbulent intensity and a high data rate. On the other hand, the effects of bias (including velocity bias and fringe bias) must be taken into consideration with high turbulent intensity and a low data rate.

Submitted
June, 1983

LITERATURE

1. Proceedings of International Symposium on Applications of Laser-Doppler Anemometry to Fluid Mechanics, Lisbon, 1982.

2. Proceedings of the Second International Workshop on Laser Velocimetry, W. Lafayette, 1974.

3. H.D. Thompson, W.H. Stevenson, Laser Velocimetry and Particle Sizing HPC, 1978.

4. Shen Xiong, Liu Husheng, "Laser", 10, 1982, 645-650.

5. Adrian, R.J. TSI Quarterly, Feb./Mar. Vol.IV, Issue 1, 1978.

6. Xie Sencun, Theory and Calculation of Axisymmetric Turbulent Jet Flow, Science Publishing Co., 1975.

7. Shen Xiong, Liu Huseng, "Journal of Mechanics", 1982, 5, 505-511.

[8] Giel, T. V. Jr., O. O. Barnett, Analytical and Experimental Study of statistical Bias in Laser Velocimetry, Laser Velocimetry and Particle sizing (1978), 86-99.

[9] Meyers, J. F., S. P. Wilkinson, Proc. International Symposium on Applications of LDA to Fluid Mechanics, (1982), 17. 4.

[10] TSI Anemometer Catalog, Laser Velocimetry Systems.

[11] TSI Anemometer Catalog, Hot Wire-Hot Film Anemometer Systems.

END

FILMED

9-85

DTIC